Ovary ecdysteroidogenic hormone requires a receptor tyrosine kinase to activate egg formation in the mosquito *Aedes aegypti*

Kevin J. Vogel, Mark R. Brown, and Michael R. Strand[1]

Department of Entomology, University of Georgia, Athens, GA 30602

Edited by David L. Denlinger, Ohio State University, Columbus, OH, and approved March 18, 2015 (received for review January 27, 2015)

Mosquitoes are major disease vectors because most species must feed on blood from a vertebrate host to produce eggs. Blood feeding by the vector mosquito *Aedes aegypti* triggers the release of two neurohormones, ovary ecdysteroidogenic hormone (OEH) and insulin-like peptides (ILPs), which activate multiple processes required for egg formation. ILPs function by binding to the insulin receptor, which activates downstream components in the canonical insulin signaling pathway. OEH in contrast belongs to a neuropeptide family called neuroparsins, whose receptor is unknown. Here we demonstrate that a previously orphanized receptor tyrosine kinase (RTK) from *A. aegypti* encoded by the gene *AAEL001915* is an OEH receptor. Phylogenetic studies indicated that the protein encoded by this gene, designated AAEL001915, belongs to a clade of RTKs related to the insulin receptor, which are distinguished by an extracellular Venus flytrap module. Knockdown of *AAEL001915* by RNAi disabled OEH-mediated egg formation in *A. aegypti*. AAEL001915 was primarily detected in the mosquito ovary in association with follicular epithelial cells. Both monomeric and dimeric AAEL001915 were detected in mosquito ovaries and transfected *Drosophila* S2 cells. Functional assays further indicated that OEH bound to dimeric AAEL001915, which resulted in downstream phosphorylation of Ak strain transforming factor (Akt). We hypothesize that orthologs of AAEL001915 in other insects are neuroparsin receptors.

insect | vector | reproduction | mosquito | oogenesis

Mosquitoes (family Culicidae, order Diptera) are of interest because several species transmit pathogens that cause disease in humans and other vertebrates. This feature of mosquito biology is due to all vector species being anautogenous, which means an adult female must blood feed at least once on a vertebrate host for each clutch of eggs she produces (1, 2). In turn, multiple cycles of blood feeding and egg formation create opportunities for transmission of pathogens between hosts.

Regulation of egg formation is best understood in *Aedes aegypti*, which is the primary vector of the viruses that cause yellow fever, dengue fever, and chikungunya in humans. Females produce no eggs in the absence of blood feeding, whereas blood feeding triggers medial neurosecretory cells in the brain to release ovary ecdysteroidogenic hormone (OEH) and several insulin-like peptide (ILP) family members including ILP3 (3–5). Both hormones induce the ovaries to produce ecdysteroid hormone (ECD), which stimulates the fat body to produce the yolk protein vitellogenin that is packaged into oocytes (3, 6, 7). OEH more strongly stimulates yolk uptake by oocytes than ILP3, whereas ILP3 but not OEH stimulates digestion of the blood meal, which provides nutrients for yolk biosynthesis (8, 9). Amino acid sensing through the target of rapamycin (TOR) pathway also enhances OEH, ILP, and ECD activity (8, 10, 11). Upon completion of yolk packaging and chorion formation, females fertilize and oviposit a clutch of 120–150 mature eggs ~3 d postblood meal (pbm).

Experimental studies in other species (12) together with identification of OEH and ILP orthologs in all mosquito genomes examined to date support a conserved role for these neurohormones in egg formation (9, 13). Studies in *A. aegypti* also establish that ILP3 activity depends upon binding to the insulin receptor (IR), a receptor tyrosine kinase (RTK), which triggers phosphorylation of downstream components in the insulin signaling pathway including Akt (4, 9, 14). OEH in contrast belongs to a poorly characterized family of neuropeptides known only from arthropods called neuroparsins (13, 15, 16). Limited sequence similarity with vertebrate insulin growth factor binding proteins initially suggested that neuroparsins function as ILP binding proteins, which could affect ILP binding to the IR and downstream signaling (15, 17). Our own results, however, indicate that OEH does not bind to ILP3 or the IR (9). Disrupting IR function using a pharmacological agonist or RNA interference (RNAi) also strongly disables ILP3 activity but has no effect on OEH (9, 11). However, intriguingly, OEH triggers phosphorylation of downstream components associated with the insulin signaling pathway including Akt (9). Taken together, these findings suggest OEH activates the insulin signaling pathway independently of the IR by binding to another receptor. Here, we show that OEH from *A. aegypti* is a ligand for an orphan RTK related to the IR.

Results

Phylogenetic Data Identify AAEL001915 as a Candidate OEH Receptor. Most insects including Diptera encode a single neuroparsin gene, which in mosquitoes encodes OEH (9, 15). An exception is the genus *Drosophila*, where *Drosophila mojavensis* and most other species have a recognizable neuroparsin gene and *Drosophila melanogaster* and four other closely related species do not (16). This suggests that neuroparsins have been lost from the *melanogaster* subgroup (16), which we reasoned might also be coupled with loss of a neuroparsin receptor. If correct, we further reasoned this loss could be helpful in identifying candidate neuroparsin (OEH) receptors in mosquitoes. All known peptide hormones bind three types of membrane receptors: G protein-coupled receptors

Significance

Mosquitoes are important because several species transmit pathogens that cause major diseases of humans and other vertebrates. Mosquitoes acquire and transmit pathogens because most species must consume blood from a vertebrate host to produce eggs. Thus, a promising strategy for disease control is to interfere with mosquito reproduction. Blood feeding triggers the release of ovary ecdysteroidogenic hormone (OEH) from the mosquito brain, which is a key regulator of egg formation. To function, however, OEH must bind a receptor, which was previously unknown. Here we identify an OEH receptor and show that it is required for egg formation. Targeting OEH–receptor interactions provides opportunities for reducing mosquito reproduction and disease transmission.

Author contributions: K.J.V., M.R.B., and M.R.S. designed research, performed research, analyzed data, and wrote the paper.

The authors declare no conflict of interest.

This article is a PNAS Direct Submission.

[1]To whom correspondence should be addressed. Email: mrstrand@uga.edu.

This article contains supporting information online at www.pnas.org/lookup/suppl/doi:10.1073/pnas.1501814112/-/DCSupplemental.

(GPCRs), protein receptor kinases (PRKs), and receptor guanylyl cyclases (RGCs). We recently analyzed the genomes of *A. aegypti*, two other mosquitoes (*Anopheles gambiae* and *Culex quinquefasciatus*), *D. mojavensis*, and *D. melanogaster* to discern patterns in GPCR, PRK, and RGC evolution in Diptera (13). A total of 451 receptor genes were identified and assigned to 75 clades (13). Forty-eight of these clades bound known peptide hormone or growth factor ligands, whereas 27 were "orphans" with no known ligands (13).

We began this study by examining the orphan clades to determine whether any contained orthologs from each species except *D. melanogaster*. Only one met this criterion: a group of PRKs named orphan R1 (OR1) that encode predicted RTK genes (Fig. 1*A*). Each species in the OR1 clade except *D. melanogaster* contained a single ortholog, which is named *AAEL001915* in *A. aegypti*. Our phylogeny indicated that OR1 also grouped with two other clades: the IR and homologs of human anaplastic lymphoma kinase (ALK), which in *D. melanogaster* is implicated in development, learning, and ethanol sensitivity (18, 19) (Fig. 1*A*). Inspection of a second predicted gene (*AAEL001884*) in VectorBase together with publicly available RNAseq data (20) strongly suggested *AAEL001915* was misannotated (Fig. S1). PCR assays confirmed this by showing that *AAEL001884* and *AAEL001915* plus two upstream exons form a single gene, henceforth referred to as *AAEL001915*, which encoded a predicted 1,371-amino-acid protein with a mass of 156 kDa (Fig. 1*B* and Fig. S1). This protein contained all conserved features of RTKs (21, 22) including an extracellular region for ligand binding, a single-pass transmembrane domain, and an intracellular tyrosine kinase domain (Fig. 1*B*). It also contained 10 predicted *N*-glycosylation sites plus a Venus flytrap (VFT) module known from several proteins including a subset of RTKs in insects and other invertebrates (23, 24). Quantitative real-time PCR (qRT-PCR) indicated that *AAEL001915* expression was higher in the ovaries of 5-d-old nonblood female *A. aegypti* than in the fat body and midgut (Fig. 1*C*). Following a blood meal *AAEL001915* expression in the ovaries initially increased but then declined at 48 h, which coincided with completion

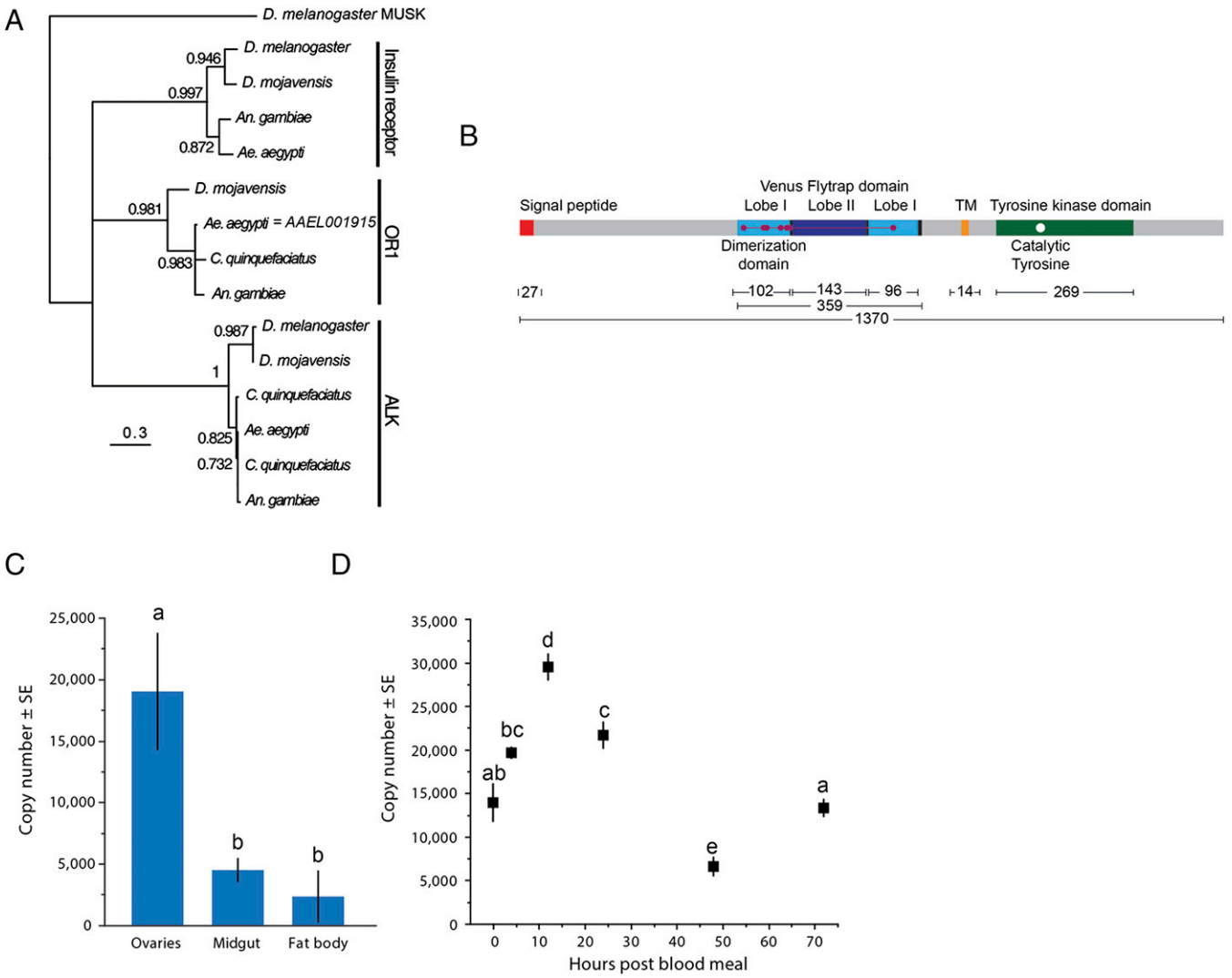

Fig. 1. *AAEL001915* is a VFT module-containing RTK that is preferentially expressed in the ovaries of blood-fed adult females. (*A*) Maximum-likelihood tree showing RTKs in the OR1, IR, and ALK clades. The tree was rooted using the muscle-specific kinase gene (MUSK) from *D. melanogaster* with support values for each branch in the tree indicated. The resulting clades form a polytomy that is distinct from all other PRK genes in dipteran genomes (13). (*B*) Domain structure of AAEL001915. The total number of amino acids in the predicted protein and select domains are indicated below the figure. The predicted transmembrane (TM) domain is indicated in yellow, the dimerization domain is indicated by red dots, and the catalytic tyrosine is indicated by a white dot. (*C*) qRT-PCR of *AAEL001915* in ovaries, midgut, and fat body from 5-d-old non–blood-fed *A. aegypti* females. Transcript abundance per 500 ng of RNA was determined from three biological and three technical replicates. Different letters above a bar indicate that transcript abundance significantly differs [$P < 0.05$, Tukey's honest significance difference (HSD) test]. (*D*) Transcript abundance of *AAEL001915* per 500 ng of RNA in ovaries from 0 to 72 h pbm. Replicates per sample and data analysis are as described in *C*.

of yolk packaging into oocytes and chorion formation (Fig. 1*D*). Transcript abundance thereafter rose at 72 h, when females oviposited mature eggs and generated secondary follicles that form eggs if a female consumes a second blood meal (Fig. 1*D*).

Knockdown of AAEL001915 Disables OEH Activity. We previously showed that dsRNA corresponding to the *A. aegypti* IR (*dsMIR*) specifically depletes this RTK in ovaries and other tissues (4, 8, 9). Likewise, injection of *dsAAEL001915* (*ds1915*) into newly emerged adult females followed by blood feeding after 5 d and qRT-PCR analysis at 48 h pbm showed that transcript abundance of *AAEL001915* was significantly reduced relative to control mosquitoes treated with *dsGFP* (Fig. S2*A*). Injection of *ds1915*, *dsMIR*, or *dsGFP* into adult females followed by blood feeding and inspection of ovaries at 48 h pbm further showed that *AAEL001915* knockdown reduced yolk deposition into oocytes more strongly than knockdown of the *MIR* (Fig. 2*A*). This finding was significant because it suggested egg formation required *AAEL001915* under conditions where OEH and ILPs are both released from brain neurosecretory cells after blood feeding. We further hypothesized this outcome was due to disrupted OEH signaling given earlier results showing that (*i*) OEH stimulates yolk uptake into oocytes more strongly than ILPs and (*ii*) ILPs but not OEH require the IR for biological activity (8, 9).

We therefore directly assessed the effects of *AAEL001915* knockdown on OEH versus ILP3 activity. Because both neurohormones stimulate the ovaries to produce ECD (4, 9), we injected non–blood-fed adult females with *ds1915* or *dsGFP*. Ovaries were then collected 5 d later and placed into medium containing OEH (330 nM) or ILP3 (400 nM) followed by measurement of ECD titers relative to ovaries in saline, which served as a negative control. These data showed that ovaries from *ds1915*-treated females produced only baseline amounts of ECD in response to OEH, whereas ILP3 strongly stimulated ECD synthesis (Fig. 2*B*). Ovaries from females treated with *dsGFP* in contrast produced elevated amounts of ECD in response to both hormones (Fig. 2*B*). We also noted that ILP3 but not OEH stimulated phosphorylation of Akt in ovaries from *ds1915*-treated females, whereas ILP3 and OEH both stimulated Akt phosphorylation in ovaries from females treated with *dsGFP* (Fig. 2*C*).

Vitellogenin synthesis by the fat body is indirectly triggered by OEH and ILP3 via ECD production and TOR signaling (6–11). We thus injected females with *ds1915* or *dsGFP*, blood fed them 5 d later as above, but then immediately decapitated each female to ablate the endogenous source of OEH and ILP3. Females were then injected with either 20 pmol of OEH or ILP3 followed by analysis of vitellogenin expression. Females treated with *ds1915* produced vitellogenin in response to ILP3 but not OEH, whereas females treated with *dsGFP* produced vitellogenin in response to both hormones (Fig. 2*D*). Inspection of the ovaries further showed no yolk uptake by oocytes in females treated with *ds1915* after injection of OEH, whereas yolk uptake increased in females treated with *dsGFP* (Fig. 2*E*). These results overall indicated that knockdown of *AAEL001915* disabled OEH but not ILP3 activation of egg formation.

AAEL001915 Dimerizes in S2 Cells and the Mosquito Ovary. Most RTKs form dimers at the cell surface (21, 22). In contrast, the IR, including from *A. aegypti*, forms covalently stabilized heterotetramers (400–500 kDa) comprised of two α subunits containing the ligand binding domain and two β subunits containing the tyrosine kinase domain (5). We cloned a full-length *AAEL001915* cDNA into the expression vector pIZT/V5-His followed by transfection into *D. melanogaster* S2 cells, which lack an OR1 ortholog. Zeocin selection was then used to produce a stably transfected cell line that constitutively expressed AAEL001915 with a C-terminal V5 epitope tag (Fig. S2*B*). We also produced an antibody (α-49) against the extracellular domain of AAEL001915 plus a second antibody (α-727) to a region near the transmembrane domain. On immunoblots, a V5 antibody (α-V5) detected a ~170 kDa band plus a second band >268 kDa in stably transfected S2 cells but

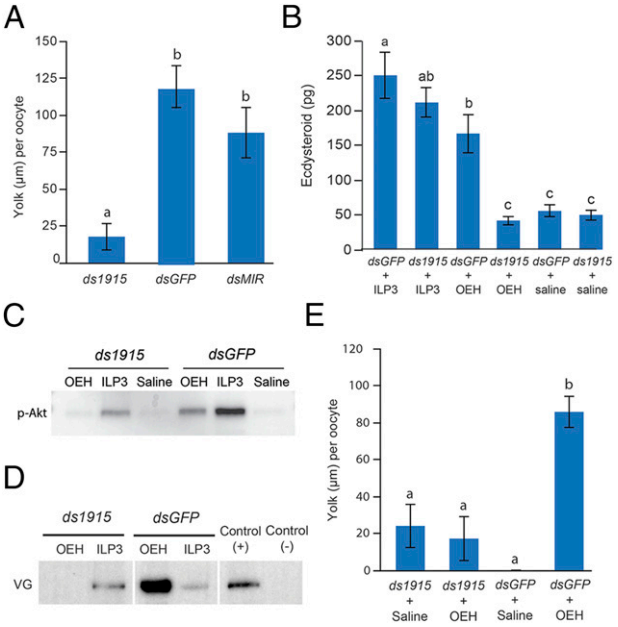

Fig. 2. Knockdown of *AAEL001915* by RNAi disables OEH but not ILP3 activation of egg formation. (*A*) Average amount of yolk per oocyte at 48 h pbm in females pretreated with *dsAAEL001915* (*ds1915*), *dsGFP*, or *dsMIR*. (*B*) ECD production by ovaries from females pretreated with *dsGFP* or *ds1915* following incubation for 6 h in Sf-900 medium plus ILP3 (330 nM), OEH (400 nM), or saline only. (*C*) Immunoblot of ovary extracts from the same treatments as shown in *B* probed with phospho-*Drosophila* Akt (Ser505), which detects ~65 kDa *A. aegypti* p-Akt (9). (*D*) Immunoblots of fat body extracts probed with an antibody that detects vitellogenin (220 kDa). Females were pretreated with *ds1915* or *dsGFP* followed by blood feeding, decapitation, and injection of either OEH (20 pmol) or ILP3 (20 pmol). Fat body samples were then processed 24 h postinjection. Fat body processed from untreated, nondecapitated females 24 h pbm served as the positive control (+), whereas fat body processed 24 h pbm from untreated females that were decapitated immediately after blood feeding served as the negative control (–). (*E*) Average amount of yolk per oocyte, as measured by yolk length, at 24 h pbm in females pretreated with *ds1915* or *dsGFP* followed by blood feeding, decapitation, and injection of OEH (20 pmol) or saline. Error bars in *A*, *B*, and *E* show 95% confidence intervals, and different letters above a given bar indicate a significant difference in response ($P < 0.05$, Tukey's HSD).

detected no bands in control cells (Fig. 3*A*). α-49 detected bands of the same mass in transfected but not control cells, while also detecting similar bands of slightly smaller mass in ovaries from blood-fed *A. aegypti* (Fig. 3*A*). The masses of these bands were consistent with AAEL001915 as a monomer and putative homodimer. The abundance of these two bands also did not strongly differ when run under nonreducing and reducing conditions (Fig. 3*A*). α-49 detected ~110 and ~60 kDa bands in ovaries that were absent in stably transfected and control S2 cells, which together had a similar mass to monomeric AAEL001915, suggesting they were cleavage products (Fig. 3*A*). α-49 also detected a doublet that ran near 41 kDa plus other bands above and below this doublet (Fig. 3*A*). However, the presence of these bands across treatments strongly suggested they reflected nonspecific binding. In immunocytochemical assays, α-727 labeled the follicular epithelium that surrounds primary and secondary follicles (Fig. 3 *B* and *C*), which is where the IR is also expressed in the mosquito ovary (25, 26). Higher magnification images suggested labeling of the follicular epithelium by α-727 was both apical and basal (Fig. 3*D*), whereas preimmune serum (negative control) detected no antigen in follicles (Fig. 3*E*).

OEH Binds to AAEL001915 and Activates Phosphosphorylation of Akt. To test whether OEH is a ligand for AAEL001915, stably transfected and control S2 cells were incubated with OEH followed by

CELL BIOLOGY

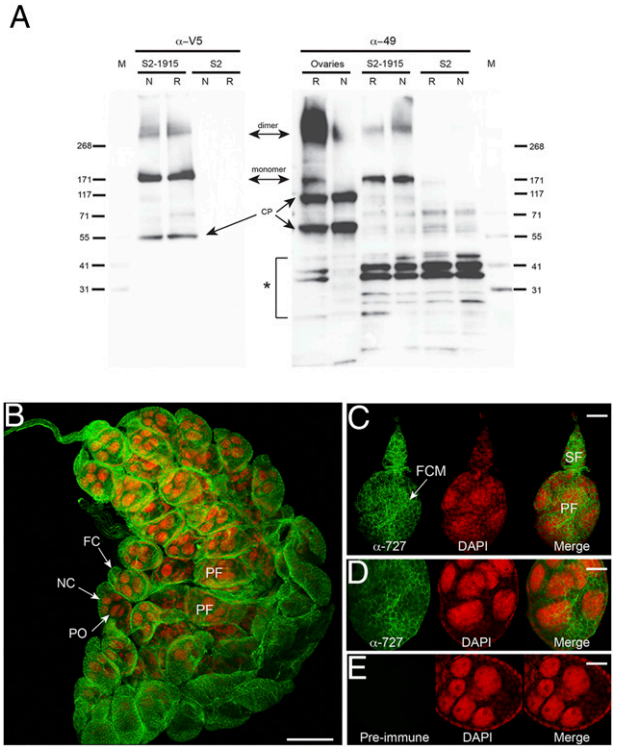

Fig. 3. Detection of AAEL001915 in *D. melanogaster* S2 cells and *A. aegypti* ovaries. (*A*) Immunoblots of extracts from S2 cells stably transfected with *pIZT/AAEL001915* (S2-1915) (5×10^5 cells per lane), control S2 cells (S2) (5×10^5 cells per lane), or ovaries (20 ovary pairs per lane). The blot on the left was probed with α-V5, whereas the blot on the right was probed with α-49. Both antibodies detected bands corresponding to monomeric and dimeric AAEL001915 in S2-1915 cells under nonreducing (N) and reducing (R) conditions. These bands are absent in control S2 cells. In ovaries, α-49 but not α-V5 detected the same bands but at a slightly smaller mass as expected in the absence of an epitope tag. A band at ∼55 kDa detected by α-V5 in S2-1915 cells plus two bands detected by α-49 in ovaries correspond to potential cleavage products (CPs) of monomeric AAEL001915. A bracket and asterisk indicate bands detected by α-49 that reflected nonspecific binding. Molecular mass markers (M) are indicated on the far left and right of the two blots. (*B–D*) Micrographs of ovaries from an *A. aegypti* female at 24 h pbm stained with α-727 (green) and DAPI (red). (*B*) A low-magnification projection, confocal image of the ovary. Representative primary follicles (PFs) are labeled. Each PF is surrounded by follicle epithelial cells (FCs) labeled with α-727 and contains an oocyte (PO) plus multiple nurse cells (NCs), whose nuclei are labeled with DAPI. (Scale bar, 100 μm.) (*C*) Intermediate magnification images of a single primary (PF) and secondary follicle (SF) plus germarium labeled with α-727 (*Left*), DAPI (*Middle*), and the merged image showing labeling with both (*Right*). α-727 labeling (green) is clearly associated with only the membrane of follicle epithelial cells (FCMs), whereas DAPI stains epithelial cell, oocyte, and nurse cell nuclei. (Scale bar, 50 μm.) (*D*) Higher magnification image showing a single optical section of a primary follicle labeled with α-727 only, DAPI, or the merged image of both. α-727 labeling of the follicle cell membranes appears both apical and basal. (Scale bar, 30 μm.) (*E*) Negative control images of a single primary follicle cell labeled with preimmune serum (*Left*), DAPI (*Middle*), or merger of both (*Right*). Only nuclei are labeled. (Scale bar, 30 μm.)

processing with or without cross-linkers. Cell extracts were then immunoblotted and probed with α-49 or a previously generated OEH antibody (α-OEH) (25). α-OEH detected a band of identical mass to dimeric AAEL001915 recognized by α-49 in transformed cells incubated with OEH (Fig. 4*A*). Signal intensity of this band was also somewhat stronger when cross-linkers were added before cell extracts were prepared (Fig. 4*A*). In contrast, α-OEH detected no band corresponding to monomeric AAEL001915 in transfected cells (Fig. 4*A*). α-OEH also detected no band corresponding to dimeric or monomeric AAEL001915 in transfected cells in the absence of OEH or in control cells with or without OEH (Fig. 4*A*). Although no neuroparsin or OR1 ortholog are endogenously present in *D. melanogaster*, the preceding result prompted us to ask whether OEH triggered phosphorylation of Akt in S2 cells expressing AAEL001915 as occurs in *A. aegypti* ovaries. We tested this by incubating transfected and control S2 cells with OEH or ILP3 as a positive control, as S2 cells express the IR and have a functional insulin signaling pathway (26–29). Strikingly, stimulation with OEH resulted in phosphorylation of Akt in S2 cells expressing AAEL001915 but not in control cells, whereas stimulation with ILP3 resulted in phosphorylation of Akt in both cell backgrounds (Fig. 4*B*). In contrast, no phosphorylated Akt (p-Akt) was detected in transfected or control cells in the absence of OEH or ILP3 (Fig. 4*B*).

Discussion

OEH was first identified in *A. aegypti* and named because it stimulates ovaries to produce ECD, which is a key step in the egg formation process following blood feeding (3). The comparative literature thereafter showed that OEH is a neuroparsin (15, 16), whereas experimental data showed that OEH and ILPs exhibit partially overlapping activity in regulating egg formation in mosquitoes (8, 9). Because OEH and ILP3 both activate downstream components of the insulin signaling cascade, we originally speculated that OEH functions by interacting with ILPs and/or the IR. Functional studies, however, strongly argued OEH functions independently of the IR by activating another receptor (9). In this study, we show that *AAEL001915* belongs to an IR-related clade of RTKs. Our functional data indicate that AAEL001915 is an OEH receptor by showing that (*i*) OEH activity in *A. aegypti* requires expression of *AAEL001915* and (*ii*) OEH binds to dimeric AAEL001915 in S2 cells, which activates downstream Akt phosphorylation through currently unknown intermediates.

As previously noted, most RTKs form noncovalent dimers, whereas the IR forms a covalently stabilized heterodimer (21, 22). Our results suggest AAEL001915 dimerizes in the mosquito ovary and S2 cells, while also showing that OEH only binds to the dimeric form of this protein. Detection of this dimer under reducing and nonreducing conditions suggests noncovalent interactions may be involved in dimerization. We hypothesize AAEL001915 forms a homodimer, but our results do not exclude the possibility AAEL001915 heterodimerizes with an unknown partner. The somewhat higher mass of AAEL001915 on gels relative to its predicted mass is likely due to glycosylation, which is characteristic of other RTKs. The increased intensity of dimeric AAEL001915 seen upon exposure to OEH could also reflect the possibility this ligand promotes receptor dimerization, which is known to occur with some other RTKs (21, 22). That OEH binding to AAEL001915 in S2 cells stimulates phosphorylation of Akt as occurs in the mosquito ovary is notable given the absence of endogenous OEH or AAEL001915 orthologs in *D. melanogaster*. On the other hand, this loss is also a relatively recent evolutionary event given the presence of neuroparsin and AAEL001915 orthologs in other drosophilids (13, 16). Thus, downstream components of the insulin signaling cascade, such as the IR substrate Chico, appear to be sufficiently conserved in *D. melanogaster* to interact with AAEL001915, whose intracellular tyrosine kinase domain structurally shares features with the IR (13, 23).

The most distinguishing feature of AAEL001915 relative to other RTKs is the VFT module in its extracellular domain. VFT modules are known from several types of membrane proteins including bacterial periplastic proteins and select GPCRs and RGCs (23). In contrast, VFT modules are unknown in PRKs, with the exception of a subset of RTKs in arthropods and select other invertebrate phyla recently named the Venus Kinase Receptor family (23, 30). All genes in the OR1 clade of our dipteran phylogeny are members of this assemblage. Examination of all sequenced insect genomes further suggests most insects outside the *melanogaster* subgroup, the lepidopteran *Bombyx mori* (23), and potentially aphids (31) contain one *AAEL001915*

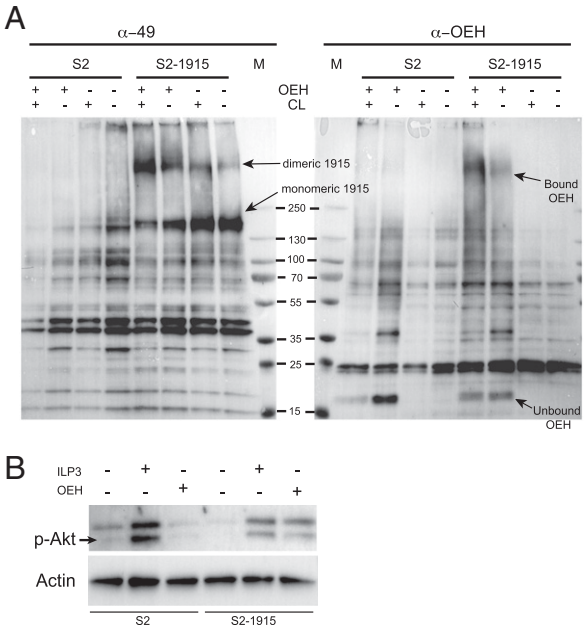

Fig. 4. OEH binds to dimeric AAEL001915 expressed in *Drosophila* S2 cells and induces phosphorylation of Akt. (*A*) Immunoblots of extracts from control (S2) and stably transfected cells expressing AAEL001915 (S2-1915) probed with α-49 (*Left*) or α-OEH (*Right*). α-49 detected monomeric and dimeric AAEL001915 in transfected but not control S2 cells, with signal intensity for the dimeric band being stronger in transfected cells exposed to OEH. α-OEH detected a band corresponding to dimeric AAEL001915 in extracts from transfected S2 cells incubated with OEH with or without a cross-linker. α-OEH also detected unbound OEH in both transfected and control S2 cells. Bands associated with nonspecific binding of α-49 present across treatments are similar to Fig. 3*A*. Several bands associated with nonspecific binding of α-OEH are also detected. (*B*) Immunoblot of total protein extracts from control (S2) and transfected (S2-1915) cells probed with an antibody that detects p-Akt. Cells (5×10^5 per lane) were incubated with (+) or without (–) OEH (40 pmol) or ILP3 (40 pmol) for 30 min before extract preparation. As the loading control, blots were also probed with an antibody to actin.

ortholog, which assembles into a phylogeny with strong branch support indicative of its relatedness (Fig. S3).

Outside of results reported here, the biological function of *AAEL001915* orthologs in arthropods that also encode a neuroparsin is unknown. Interestingly however, studies of the distantly related trematode *Schistosoma mansoni* identifies two VFT-containing RTKs, *Smvkr1* and *Smvkr2*, which are preferentially expressed in ovaries (32). Knockdown of these genes by RNAi also disables egg formation (32, 33). The native ligand(s) for these receptors is unknown, although expression in *Xenopus* oocytes indicates L-arginine and calcium activate SmVKR1 and downstream signaling of the PI3K/Akt/S6K pathway (33). An in vitro assay also showed that L-arginine stimulated phosphorylation of a VFT-containing RTK from the honey bee, *Apis mellifera*, expressed in a human cell line (23). In contrast, our results argue against amino acids or calcium activating AAEL001915, given the media (Sf-900 or SFX) used in our in vitro experiments contain an abundance of both, yet ovaries produce no ECD and S2 cells show no evidence of Akt phosphorylation in the absence of OEH or ILP3 (Figs. 2 and 4). Hemolymph from mosquitoes and other insects also contains an abundance of free amino acids (34), but multiple experiments in *A. aegypti* and other mosquitoes indicate that ECD biosynthesis, vitellogenin production, and yolk packaging into oocytes never occur unless activated by OEH and/or ILPs (4, 8, 9, 12).

Identification of AAEL001915 as an OEH receptor in *A. aegypti* fills a critical gap in understanding how OEH and ILPs interact to activate ECD production and whether oocytes uptake yolk in direct or indirect response to these hormones. Identification of AAEL001915 could also advance our understanding of neuroparsin function, which outside of OEH and mosquitoes is poorly understood. A shrimp neuroparsin was recently shown to be provitellogenic (35), which is similar to the activity of OEH. In contrast, studies from locusts suggest neuroparsins have multiple functions (16, 17), whereas the loss of neuroparsins from the *melanogaster* subgroup argues these factors may be dispensable due potentially to overlap with ILP function (16).

Methods

Mosquitoes, Cell Culture, and Neurohormones. All experiments were conducted using the UGAL strain of *A. aegypti*, which was reared as described (9). S2 cells from *D. melanogaster* were maintained at 27 °C in serum-free SFX medium (HyClone) (36). Recombinant *A. aegypti* OEH (18,278 Da) was produced and purified as described (8, 9). *A. aegypti* ILP3 (5,850 Da) was synthesized and purified by CPC Scientific as reported (4). Both neurohormones were diluted from frozen stocks for use in bioassays.

Phylogenetic and Domain Structure Analyses. *AAEL001915* orthologs were identified via BLASTp searches against the National Center for Biotechnology Information non-redundant (NCBI nr) database. Protein sequences were aligned using the multiple sequence alignment by fast fourier transform (MAFFT) program (37) and curated using Jalview (38). Maximum likelihood phylogenies were constructed using full-length sequences and the PhyML server using default parameters (39). Trees were visualized in FigTree (tree.bio.ed.ac.uk/software/figtree/). Predicted *N*-glycosylation sites were identified using the NetNGlyc 1.0 Server (www.cbs.dtu.dk/services/NetNGlyc/). Outward-facing primers were designed for each predicted exon and untranslated region of *AAEL001884* and *AAEL001915* (Table S1) and used in PCR assays with genomic DNA or ovary cDNA as the template. The full-length coding sequence for the correctly annotated *AAEL001915* gene was amplified using primers located in the 5′ and 3′ UTRs (Table S1), followed by cloning into pSC-A (Agilent) and sequencing (Macrogen) using primers listed in Table S1.

qRT-PCR Assays. Ovaries, fat body, and midgut were dissected from 5-d-old non–blood-fed females, whereas ovaries were collected at selected time points 0–72 h pbm. RNA was extracted from samples using the High Pure RNA extraction kit (Roche) and reverse transcribed using the iSCRIPT cDNA synthesis kit and 500 ng of total RNA (Bio-Rad). qRT-PCR was performed using Rotor-Gene qPCR reagents (Qiagen) with standards (40).

RNAi. A 459 bp fragment of AAEL001915 was chosen for dsRNA synthesis. Primers including the consensus T7 promoter sequence (Table S1) were used to amplify the target from 24 h pbm ovary cDNA. PCR products were then used in the MegaScript RNAi kit (Life Technologies), followed by ethanol precipitation and resuspension in saline at 4 μg/μL. Double-stranded RNAs corresponding to enhanced GFP or the *A. aegypti* IR were similarly produced (4, 8). Newly emerged adult female mosquitoes were injected with 4 μg of dsRNA in 1 μl saline and then held in humidified chambers with 5% sucrose (wt/vol) for 24 h and thereafter water. For yolk deposition and ECD assays, mosquitoes were blood fed 5 d postinjection with dsRNA and then dissected 48 h later for ovary collection. For rescue experiments, mosquitoes were blood fed 5 d posttreatment, immediately decapitated, and injected with saline or saline containing 20 pmol of OEH or ILP3 followed by analysis of yolk deposition or vitellogenin biosynthesis.

Yolk Deposition, ECD Biosynthesis, Vitellogenin, and Akt Expression. We estimated yolk deposition by examining ovaries from dissected females under a stereomicroscope and then measuring along the long axis the length of yolk per oocyte in μm using an ocular micrometer (4, 8). ECD biosynthesis by ovaries was measured by RIA after incubation for 6 h in 60 μL of Sf-900 medium (Invitrogen) plus OEH (330 nM = 20 pmol/60 μL), ILP3 (400 nM = 20 pmol/60 μL), or saline with no hormone before processing (41). The antibody used in the assay recognizes ecdysone and 20-hydroxyecdysone equally (41). Activation of Akt was assessed by incubating ovaries under the same conditions for 30 min followed by processing and immunoblotting using the phospho-*Drosophila* Akt (Ser505) antibody as described below. Vitellogenin was analyzed by immunoblotting using homogenates of abdomen walls with attached fat body in water and Laemmli sample buffer (1:1) without a reducing agent (12). Samples were electrophoresed on 4–20% acrylamide (wt/vol), Tris·HCl gels (Lonza) (100 μg per lane) followed by transfer to PVDF (Whatman). Blots were probed with a rabbit antibody to *A. aegypti* vitellogenin (R2, 1:100,000) and a peroxidase-conjugated goat anti-rabbit

secondary antibody (Jackson; 1:10,000) followed by visualization using a chemiluminescent substrate (ECL Advance, GE Healthcare) (12).

S2 Cell Transfection. Full-length *AAEL001915* was PCR amplified using specific primers (Table S1) and ovary cDNA as the template followed by directional cloning into pIZT/V5-His (Invitrogen), which uses the OpIE2 promoter from the *Orgyia pseudotsugata* baculovirus for constitutive expression and encodes a Zeocin-green fluorescent protein (GFP) gene fusion under the OpIE1 promoter. *AAEL001915* cloned in frame with the V5-6xHis epitope tag was confirmed by sequencing. This plasmid was then transfected into S2 cells followed by Zeocin selection as previously described (36, 42).

Detection of Akt and AAEL001915. p-Akt was detected in *A. aegypti* ovaries and S2 cells using a phospho-*Drosophila* Akt (Ser505) antibody (Cell Signaling) and previously established immunoblotting conditions (9). This antibody only visualizes p-Akt in *A. aegypti* (9), whereas it recognizes p-Akt and a second higher mass band in S2 cells (Cell Signaling). An anti-actin antibody (Sigma) served as a loading control. Two affinity-purified antibodies (α-49, α-727) were commercially produced (GeneScript) in rabbits against AAEL001915 corresponding to amino acids 49–63 (KENQLPRFASRNQN) and amino acids 727–740 (RRHSYMESDYAGYA). Ovary and S2 cell homogenates were prepared in a protease inhibitor mixture, and protein concentrations were determined by Bradford assay. Samples were electrophoresed as above (100 μg per lane) in Laemmli buffer with or without 2 mercaptoethanol (10 μM). Following transfer to PVDF, immunoblots were processed as described above using α-49 (1:1,000) as the primary antibody. AAEL001915 was visualized immunocytochemically by fixing ovaries from *A. aegypti* females 24 h pbm with 4% paraformaldehyde (wt/vol). Samples were permeabilized with 0.5% Triton X-100 in PBS, blocked using 5% goat serum (vol/vol), and incubated with α-727 (1:100) overnight at 4 °C. Following multiple washes in PBT, ovaries were labeled with secondary antibody (1:2,000) conjugated to Alexa Fluor 488 (Molecular Probes), counterstained with the DNA labeling dye 4′,6-diamidino-2-phenylindole (DAPI), and examined using a Zeiss confocal microscope. Recombinant AAEL001915 was detected in stably transfected S2 cells using α-V5 (1:500) as the primary antibody and Alexa Fluor 560 as the secondary antibody.

OEH Binding and Insulin Signaling Pathway Activation. Control and stably transfected S2 cells expressing AAEL001915 were transferred to microfuge tubes (5×10^5 cells per tube), gently pelleted by centrifugation, and resuspended in 70 μL of PBS alone or PBS containing 40 pmol of OEH. After 15 min at room temperature, 30 μL of PBS or PBS containing 0.15 mM of the cross-linkers BS2G and BS3 (1:1) (ProteoBiochem) was added for 60 min, followed by pelleting and resuspension in 150 μL of PBS. Protein extracts were then prepared, electrophoresed under nonreducing conditions, and transferred to PVDF followed by immunoblotting using α-49 or α-OEH (1:10,000) (25). Activation of Akt was assessed by incubating control and stably transfected cells under the same conditions for 30 min, followed by processing and immunoblotting using the phospho-*Drosophila* Akt (Ser505) antibody as described above.

ACKNOWLEDGMENTS. We thank A. Elliot and S. Robertson for assistance in rearing and dissecting mosquitoes, D. A. McKinney for assistance with radioimmunoassays, B. J. Yates and S. A. Thomas for assistance with qRT-PCR, and J. A. Johnson for assistance with microscopy. This study was sponsored by National Institutes of Health Grants R01AI033108 (to M.R.B. and M.R.S.) and F32GM109750 (to K.J.V.).

1. Briegel H (2003) Physiological bases of mosquito ecology. *J Vector Ecol* 28(1):1–11.
2. Clements AN (1992) *The Biology of Mosquitoes* (Chapman & Hall, London), Vol 1.
3. Brown MR, et al. (1998) Identification of a steroidogenic neurohormone in female mosquitoes. *J Biol Chem* 273(7):3967–3971.
4. Brown MR, et al. (2008) An insulin-like peptide regulates egg maturation and metabolism in the mosquito *Aedes aegypti*. *Proc Natl Acad Sci USA* 105(15):5716–5721.
5. Wu Q, Brown MR (2006) Signaling and function of insulin-like peptides in insects. *Annu Rev Entomol* 51:1–24.
6. Attardo GM, Hansen IA, Raikhel AS (2005) Nutritional regulation of vitellogenesis in mosquitoes: Implications for anautogeny. *Insect Biochem Mol Biol* 35(7):661–675.
7. Riehle MA, Brown MR (1999) Insulin stimulates ecdysteroid production through a conserved signaling cascade in the mosquito *Aedes aegypti*. *Insect Biochem Mol Biol* 29(10):855–860.
8. Gulia-Nuss M, Robertson AE, Brown MR, Strand MR (2011) Insulin-like peptides and the target of rapamycin pathway coordinately regulate blood digestion and egg maturation in the mosquito *Aedes aegypti*. *PLoS ONE* 6(5):e20401.
9. Dhara A, et al. (2013) Ovary ecdysteroidogenic hormone functions independently of the insulin receptor in the yellow fever mosquito, *Aedes aegypti*. *Insect Biochem Mol Biol* 43(12):1100–1108.
10. Roy SG, Hansen IA, Raikhel AS (2007) Effect of insulin and 20-hydroxyecdysone in the fat body of the yellow fever mosquito, *Aedes aegypti*. *Insect Biochem Mol Biol* 37(12):1317–1326.
11. Roy SG, Raikhel AS (2011) The small GTPase Rheb is a key component linking amino acid signaling and TOR in the nutritional pathway that controls mosquito egg development. *Insect Biochem Mol Biol* 41(1):62–69.
12. Gulia-Nuss M, Eum J-H, Strand MR, Brown MR (2012) Ovary ecdysteroidogenic hormone activates egg maturation in the mosquito Georgecraigius atropalpus after adult eclosion or a blood meal. *J Exp Biol* 215(Pt 21):3758–3767.
13. Vogel KJ, Brown MR, Strand MR (2013) Phylogenetic investigation of peptide hormone and growth factor receptors in five dipteran genomes. *Front Endocrinol (Lausanne)* 4:193.
14. Wen Z, et al. (2010) Two insulin-like peptide family members from the mosquito *Aedes aegypti* exhibit differential biological and receptor binding activities. *Mol Cell Endocrinol* 328(1-2):47–55.
15. Badisco L, et al. (2007) Neuroparsins, a family of conserved arthropod neuropeptides. *Gen Comp Endocrinol* 153(1-3):64–71.
16. Veenstra JA (2010) What the loss of the hormone neuroparsin in the *melanogaster* subgroup of *Drosophila* can tell us about its function. *Insect Biochem Mol Biol* 40(4):354–361.
17. Claeys I, et al. (2006) Neuroparsin transcripts as molecular markers in the process of desert locust (*Schistocerca gregaria*) phase transition. *Biochem Biophys Res Commun* 341(2):599–606.
18. Gouzi JY, et al. (2011) The receptor tyrosine kinase Alk controls neurofibromin functions in *Drosophila* growth and learning. *PLoS Genet* 7(9):e1002281.
19. Lasek AW, et al. (2011) An evolutionary conserved role for anaplastic lymphoma kinase in behavioral responses to ethanol. *PLoS ONE* 6(7):e22636.
20. Akbari OS, et al. (2013) The developmental transcriptome of the mosquito Aedes aegypti, an invasive species and major arbovirus vector. *G3 (Bethesda)* 3(9):1493–1509.
21. Lemmon MA, Schlessinger J (2010) Cell signaling by receptor tyrosine kinases. *Cell* 141(7):1117–1134.
22. Biarc J, Chalkley RJ, Burlingame AL, Bradshaw RA (2011) Receptor tyrosine kinase signaling—A proteomic perspective. *Adv Enzyme Regul* 51(1):293–305.
23. Ahier A, et al. (2009) A new family of receptor tyrosine kinases with a venus flytrap binding domain in insects and other invertebrates activated by aminoacids. *PLoS ONE* 4(5):e5651.
24. Felder CB, Graul RC, Lee AY, Merkle HP, Sadee W (1999) The Venus flytrap of periplasmic binding proteins: An ancient protein module present in multiple drug receptors. *AAPS PharmSci* 1(2):E2.
25. Graf R, Neuenschwander S, Brown MR, Ackermann U (1997) Insulin-mediated secretion of ecdysteroids from mosquito ovaries and molecular cloning of the insulin receptor homologue from ovaries of bloodfed *Aedes aegypti*. *Insect Mol Biol* 6(2):151–163.
26. Riehle MA, Brown MR (2002) Insulin receptor expression during development and a reproductive cycle in the ovary of the mosquito *Aedes aegypti*. *Cell Tissue Res* 308(3):409–420.
27. Brown MR, Cao C (2001) Distribution of ovary ecdysteroidogenic hormone I in the nervous system and gut of mosquitoes. *J Insect Sci* 1:3.
28. Puig O, Tjian R (2005) Transcriptional feedback control of insulin receptor by dFOXO/FOXO1. *Genes Dev* 19(20):2435–2446.
29. Hietakangas V, Cohen SM (2007) Re-evaluating AKT regulation: Role of TOR complex 2 in tissue growth. *Genes Dev* 21(6):632–637.
30. Dissous C, Morel M, Vanderstraete M (2014) Venus kinase receptors: Prospects in signaling and biological functions of these invertebrate kinases. *Front Endocrinol (Lausanne)* 5:72.
31. Huybrechts J, et al. (2010) Neuropeptide and neurohormone precursors in the pea aphid, *Acyrthosiphon pisum*. *Insect Mol Biol* 19(Suppl 2):87–95.
32. Vicogne J, et al. (2003) An unusual receptor tyrosine kinase of *Schistosoma mansoni* contains a Venus Flytrap module. *Mol Biochem Parasitol* 126(1):51–62.
33. Vanderstraete M, et al. (2014) Venus kinase receptors control reproduction in the platyhelminth parasite *Schistosoma mansoni*. *PLoS Pathog* 10(5):e1004138.
34. Munkirs DD, Christensen BM, Tracy JW (1990) High-pressure liquid chromatographic analysis of hemolymph plasma catecholamines in immune-reactive *Aedes aegypti*. *J Invertebr Pathol* 56(2):267–279.
35. Yang SP, He J-G, Sun CB, Chan SF (2014) Characterization of the shrimp neuroparsin (MeNPLP): RNAi silencing resulted in inhibition of vitellogenesis. *FEBS Open Bio* 4:976–986.
36. Pruijssers A, Strand MR (2007) PTP-H2 and PTP-H3 from Microplitis demolitor Bracovirus localize to focal adhesions and are antiphagocytic in insect immune cells. *J Virol* 81(3):1209–1219.
37. Katoh K, Kuma K, Toh H, Miyata T (2005) MAFFT version 5: Improvement in accuracy of multiple sequence alignment. *Nucleic Acids Res* 33(2):511–518.
38. Waterhouse AM, Procter JB, Martin DMA, Clamp M, Barton GJ (2009) Jalview Version 2—A multiple sequence alignment editor and analysis workbench. *Bioinformatics* 25(9):1189–1191.
39. Guindon S, et al. (2010) New algorithms and methods to estimate maximum-likelihood phylogenies: Assessing the performance of PhyML 3.0. *Syst Biol* 59(3):307–321.
40. Bitra K, Suderman RJ, Strand MR (2012) Polydnavirus Ank proteins bind NF-κB homodimers and inhibit processing of Relish. *PLoS Pathog* 8(5):e1002722.
41. Sieglaff DH, Duncan KA, Brown MR (2005) Expression of genes encoding proteins involved in ecdysteroidogenesis in the female mosquito, *Aedes aegypti*. *Insect Biochem Mol Biol* 35(5):471–490.
42. Beck M, Strand MR (2005) Glc1.8 from Microplitis demolitor bracovirus induces a loss of adhesion and phagocytosis in insect high five and S2 cells. *J Virol* 79(3):1861–1870.